

# Strain Rate Effect on Crystallinity Variations in the Double Yield Region of Polyethylene

Angel Manzur

Departamento de Física, Universidad Autónoma Metropolitana-Iztapalapa, Apartado Postal 55-534, 09340 México, D. F., México

Received 21 June 2007; accepted 23 November 2007

DOI 10.1002/app.27806

Published online 28 January 2008 in Wiley InterScience (www.interscience.wiley.com).

**ABSTRACT:** The double yield phenomenon was studied using numerous specimens uniaxially deformed up to different elongations of linear low-density polyethylene samples. Extruded samples prepared under different conditions were deformed at 1, 10, and 50 mm/min. The crystallinity under stressed state was calculated using the wide-angle X-ray scattering technique. The crystallinity degrees of the samples without deformation were less than 55%. This parameter, as a function of the elongation, presented a multistep behavior. An increment before the first yield point and a decrement after this point; then, at higher elongation values around the second yield point,

another decrement and an abrupt increment. The behavior was more notorious at intermediate and lower strain rates. The results around the second yield point were interpreted in terms of melting of the less perfect crystallites followed by a recrystallization process. These experimental findings show that the partial melting–recrystallization process is one of the main mechanisms of the double yield phenomenon. © 2008 Wiley Periodicals, Inc. *J Appl Polym Sci* 108: 1574–1581, 2008

**Key words:** linear low-density polyethylene; stress–strain; crystallinity; melting–recrystallization

## INTRODUCTION

A general definition of yield is the point at which a material ceases to deform elastically in a recoverable manner and undergoes permanent (irreversible) plastic deformation. A yield point in polymers appears as a local maximum in the stress–strain curve. The yielding phenomenon of semicrystalline polymers is associated with a morphological change where a spherulitic structure transforms into a fibrillar one.<sup>1–3</sup>

Experimental evidence published for polyethylene (PE) under tensile loading has shown that two yield points exist.<sup>4–16</sup> This double yield phenomenon depends critically on a number of factors and has been analyzed (a) in several systems: PE and related copolymers, binary and ternary blends; (b) in PEs with a variety of properties: linear or branched, different molecular weight, crystal thickness distributions, and crystallinity; (c) under distinct experimental conditions: deformation temperature and strain rate; and (d) in samples with different thermal history.

The same general scenario of double yielding has also been seen in other polymeric systems such as poly(tetramethylene terephthalate) and related copolymers,<sup>17</sup> polyamide 6 and its composites,<sup>18,19</sup>

polybutylene terephthalate,<sup>20</sup> polypropylene,<sup>11</sup> and polycarbonate/polyethylene (PC/PE) blends.<sup>21–23</sup> It was thought for many years that this phenomenon is a characteristic manifested only in semicrystalline polymers. However, double yielding, similar to that observed in some semicrystalline polymers, was detected in nanostructured amorphous polymer.<sup>24</sup>

Experiments show that the stress–strain curve in the double yield region may have comparable magnitudes of the stress of both maxima or a predominant value of one of them. The first yield maximum is preponderant under extreme conditions of low temperatures, high strain rates, or high crystallinity. The second maximum does under the opposite extreme conditions. It is expected that different deformation mechanisms exist for each yield maximum. However, the given interpretation has not been unique, possibly, because several mechanisms are involved.

Some models and mechanisms have been given to explain the origin of the double yield phenomenon. For example, it has been proposed that the onset of plastic deformation in semicrystalline polymers is governed by two structurally well-defined processes: a slip of the crystal blocks past each other in the mosaic crystalline structure and a homogeneous shear of the crystal blocks.<sup>5,7,10,25</sup> These characteristics were discussed with regard to two thermally activated rate processes of plastic deformation.<sup>7</sup> Results from tensile experiments<sup>6,14</sup> at room temperature, showed that the mechanism operating at the

Correspondence to: A. Manzur (amg@xanum.uam.mx).

first yield point marked the beginning of plastic strains which are slowly recoverable, whereas the mechanism that governs the second yield point brings a truly plastic strain and was associated with a sharp necking of the samples. The two yield points have been interpreted mechanically as the yield of two dashpots, and the model used to describe the yield is of two Voigt elements in series,<sup>10</sup> two non-linear Maxwell elements in parallel,<sup>6</sup> or as two distinct thermally activated rate processes.<sup>26</sup>

Other proposed explanation for the mechanisms involved in the double yield phenomenon was reported.<sup>4,8</sup> From the experimental findings in a set of linear PEs and well-characterized ethylene copolymers of narrow molecular weight and composition distribution, and varying molecular weight, initial crystallinity, strain rate, and temperature, a qualitative explanation was based on the postulate of a partial melting–recrystallization process during deformation. This model had been questioned by the absence of experimental evidence of partial melting during tensile deformation, and by the fact that it presupposed that the polymer must have a wide distribution of lamellar thickness.<sup>5,7,12</sup> Respect to this interpretation, a recent study was reported on the variations of the degree of crystallinity and mean crystal size as functions of uniaxial elongation in the double yield behavior of a linear low-density polyethylene (LLDPE). Wide-angle X-ray scattering (WAXS) was utilized and the results showed a decrease and then an increase of the degree of crystallinity around the second yield point, suggesting that indeed melting and recrystallization occurs in this region.<sup>27</sup> The mean size of crystallites also detected the partial melting.

It is important to emphasize that the models developed for describing the double yielding processes in semicrystalline polymers cannot be directly applied to an amorphous polymer<sup>24</sup> and to an amorphous/semicrystalline blend.<sup>22</sup> The double yielding behavior was observed in a nanostructured amorphous polymer involving a highly asymmetric styrene/butadiene star-block copolymer of polystyrene (PS) and random poly(styrene-*co*-butadiene) (PS-*co*-PB) copolymer.<sup>24</sup> It was suggested that the first yield point might be caused by the deformation of the styrene chains present in or mixed into the PS-*co*-PB random copolymer. The second yield point may be correlated to the permanent plastic flow (micro-necking and yielding) of the pure PS domains. In the case of an amorphous/semicrystalline blend, the immiscible PC/PE blend underwent double yielding.<sup>21–23</sup> It was observed that the double yielding points are morphology-dependent, with the first one by the result of the yielding of PE, and the second one caused by the yielding of amorphous PC fibers.

This work complements a previous study that had a similar objective.<sup>27</sup> The connections of the two

studies will become clear from the results of this study. This research focused on a study of the changes of the crystallinity degree during deformation in the double yield region of a LLDPE. Because melting and recrystallization occurs around the second yield maximum and the entire double yield phenomenon strongly depends on the strain rate, variations in the crystallinity behavior are expected when the strain rate is varied. Three strain rates were used which correspond to the cases when the first yield maximum is dominant, the two maxima have similar magnitudes, and the second maximum is dominant. The double yield behavior was analyzed by evaluating the crystallinity as a function of uniaxial elongation using WAXS. Since there is a strong correlation between the nature of the yield region and the permanent deformation of the material, the results of this investigation should set the basis for the understanding of the deformation process in the double yield region.

## EXPERIMENTAL

### Mechanical testing specimens

The LLDPE was acquired from Dow Chemical (Dowlex 2101), which has a melt index of 1.6 dg/min, a density of 0.924 g/cm<sup>3</sup>, and was used without any modification. Three sheets with a uniform average thickness of 1.1 mm were prepared using a single-screw Brabender extruder. The temperatures at the different zones (2 in the barrel and 1 in the die) were set at the fixed value of 150 or 180°C, and the extruder's screw was adjusted at the fixed angular speed of 40 or 70 rpm. These three samples are referred to as 150/40, 150/70, and 180/70. From the sheets, specimens with the standard dumbbell shape with a central average width of 7.5 mm were punched out for tensile tests.

The uniaxial stretching experiments were performed at room temperature (25°C) in a tensile testing machine (Instron, model 4502, Canton, MA). The clamp-to-clamp distance was fixed at 27.0 mm. To establish the adequate crosshead speeds at which the two yield points are well-defined and one maximum is dominant or both maxima have comparable values of yield stress, experiments were done at different deformation rates. The specimens were stretched with a fixed deformation rate of 1, 10, or 50 mm/min up to predetermined elongations in the interval where the double yield phenomenon occurs. Each test was done using a new specimen. For the determination of the crystallinity, it is necessary to maintain the sample in the stressed state (SS) to prevent the relaxation that inevitably occurs after removing the load. A special X-ray sample-holder, built for this purpose, was placed near the center of

the stretched sample; then the sample was cut for X-ray analysis. Specimens 150/40 were deformed at 1 mm/min, those 150/70 at 10 mm/min and 180/70 at 50 mm/min, i.e., each sample prepared under a particular processing condition was stretched at a fixed rate. In the text the samples are referred indistinctly as the processing condition or as the stretching rate.

### WAXS measurements

WAXS spectra were recorded with the aid of a horizontal goniometer (Philips, model PW 1380/60, Eindhoven, The Netherlands) fitted with a scintillation counter, pulse-height analyzer, and a graphite crystal monochromator placed in the scattered beam. Cu K $\alpha$  radiation was generated at 30 kV and 20 mA. The scans of the angular position ( $2\theta$ ) were carried out at the rate of  $1^\circ/\text{min}$ , and the scattered radiation was registered in the interval from  $5^\circ$  to  $35^\circ$ . The WAXS measurements were recorded in the equator direction; that is, with the elongation axis of the stretched specimen held perpendicular to the plane defined by the incident beam and direction of scanning. In all cases, around 10 min was spent between the end of the stretching experiment and the beginning of the WAXS experiment. After the subtraction of the background scattering and smoothing each pattern, deconvolution using Lorentzian functions was applied to separate the contribution of amorphous and crystalline parts in the angular range from  $15.0^\circ$  to  $27.5^\circ$ .

### DSC measurements

Differential scanning calorimetry (DSC) was used to confirm the crystallinity of the samples in the unstrained state. Measurements were taken on a DSC (TA Instruments, model 2920, New Castle, DE). Samples weighing about 6–7 mg were loaded into standard aluminum pans. The scans were carried out at  $10^\circ\text{C}/\text{min}$  and under nitrogen atmosphere. The percent crystallinity was calculated from the specific heat of fusion by taking the specific heat of fusion of perfectly crystalline PE to be  $293 \text{ J/g}$ .<sup>28</sup>

## RESULTS AND DISCUSSION

### Stress–strain

The samples exhibited the nominal stress–strain curves ( $\sigma$ – $\varepsilon$ ) shown in Figure 1. Each curve has a different shape. A yield maximum appears at the highest stretching rate. On its right-hand side, a hump takes place and develops with decreasing stretching rate to a second maximum at the stretching rate of 10 mm/min; at this intermediate rate the stress value of this second yield maximum becomes com-

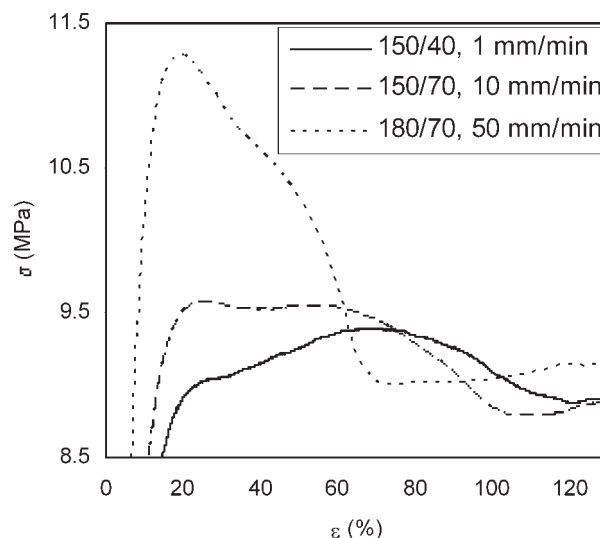


**Figure 1** Nominal stress–strain curves in the double yield region, for the three stretching rates.

parable to that of the first maximum, then this second, broader maximum becomes predominant at the smaller stretching rate. In the figure, it is clear that at higher stretching rate the PE has higher yield stress and the elongation range for the double yield region is smaller. The stress relaxation has been used to explain these effects.<sup>13</sup> When the deformation takes place rapidly, the effect of the stress relaxation is small; however, when the deformation is applied slowly, the stress value is smaller because the relaxation has enough time to reduce the stress. Visual observations of the deformation process also detected the onset of necking around the second yield, as reported.<sup>6–8,12,27</sup>

Two other important factors that may affect the shape of the curves shown in Figure 1 are the combined effects of the initial crystallinity degree and the deformation rate. Because of the different thermal history caused by the processing conditions, samples 150/40, 150/70, and 180/70 without deformation had WAXS crystallinity of 52.6, 54.5, and 45.3%, respectively. From the specific heat of fusion values, the degrees of crystallinity  $\Phi_{\text{DSC}}$  were calculated to be 46.2, 47.1, and 44.4%. These crystallinity values differ from those obtained using the WAXS technique. It is known that different experimental crystallinity measurement may give different values.<sup>29</sup> However, both techniques confirm the order of the crystallinity values of the samples, i.e., the DSC result is in accordance with the WAXS test.

Because the crystallinity values for samples processed at  $150^\circ\text{C}$  are very close to each other and that processed at the higher temperature has the smallest crystallinity value, and since the stress increases with crystallinity, it would be expected that sample 180/70 had the smallest stress if the samples were

deformed at the same rate. Therefore, due to the values used for these two factors (initial crystallinity and stretching rate), the deformation rate has the greater effect because these three samples cover a relative small range of the initial crystallinity.

The behavior of curves displayed in Figure 1 has also been obtained for PEs in a variety of experimental conditions; for example, at different values of deformation temperature, strain rate, and initial crystallinity.<sup>5-8</sup> An acute first yield point is observed for a fixed strain rate at low temperatures, but as the temperature enlarges, this gradually becomes less pronounced and a broader second yield dominates at higher temperatures. When both temperature and strain rate are varied, the first yield point is the major factor at low temperatures and high strain rates; the second yield point is more pronounced than the first one at the opposite conditions, i.e., at high temperatures and low strain rates. The effect produced by the initial crystallinity has also been analyzed at constant deformation temperature and strain rate.<sup>7,8</sup> The variations in the shape of the stress-strain curve with decreasing crystallinity degree are very similar to the variations observed with decreasing stretching rate.

## WAXS

To obtain the correlation of the changes of the mechanical properties shown in Figure 1 and the changes of the crystallinity degree, this last property was examined as a function of elongation. The relaxation effects in the SS during the WAXS experiment can be disregarded, since for a specimen stretched to an elongation of 60%, at the intermediate deformation rate of 10 mm/min, the X-ray spectra were not appreciably changed in 15 h. Figure 2 illustrates the WAXS pattern corresponding to the unstrained 150/70 sample and the changes in the pattern of one specimen strained to  $\epsilon = 61.7\%$  (in the region of the second yield point) at 10 mm/min, denoted as SS. Immediately after this run, the stress was removed (released state, RS) and a second pattern was obtained. The figure gives an example, selected from among the specimens, that shows the different shapes of the spectra that can be observed and the important effect of the deformation level. The different spectra that were obtained vary in a very systematic manner.

The spectra show the two characteristic peaks (110) and (200) of the orthorhombic crystalline structure typical of PE.<sup>29</sup> In general, as a consequence of the deformation level, the intensity of the (110) reflection in the SS slightly decreases, while that of the (200) reflection increases. After the applied stress is removed, the intensity of (110) peak becomes higher for all elongations, while the intensity for the

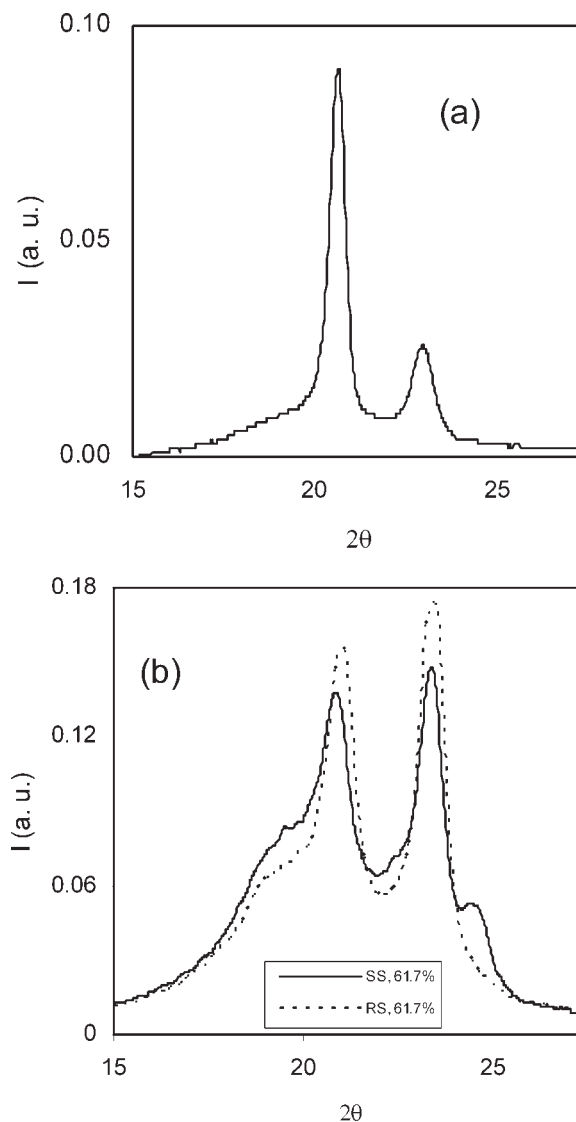


**Figure 2** WAXS spectra of 150/70 specimens stretched at 10 mm/min. (a) Unstrained specimen and (b) specimen in the stressed state (SS) at the elongation of 61.7%, and in the released state (RS) (after removal of the stress). These spectra were not smoothed.

(200) peak decreases for elongations below the second yield but increases for higher elongations. In a recent report<sup>27</sup> for 150/70 sample, it was confirmed that in the RS the intensity of the (110) reflection at the first yield point almost restores its value for the unstrained specimen, indicating that the initial properties are almost recoverable.

These intensity changes of the orthorhombic peaks may be explained by considering the orientation. It was reported for LLDPE samples that there was discernible orientation only for elongations after the first yield maximum.<sup>16,30</sup> The decrease in orthorhombic (110) intensity was directly correlated with the increase in monoclinic ( $\bar{2}01$ ) intensity. At the first yield point the orthorhombic (200) reflection oriented

rapidly toward the equator, its intensity increased up to elongations beyond the second yield maximum, but remained constant when reaching the plateau region of the  $\sigma$ - $\varepsilon$  curve.

For stretched specimens, in the second yield portion of the  $\sigma$ - $\varepsilon$  curve, a small extra reflection was registered (approximately at  $2\theta = 24.6^\circ$  for 150/70 specimens) because of the monoclinic phase, starting from the elongation about  $\varepsilon = 54.3, 50.9,$  and  $50.4\%$  for the deformation rates of 1, 10, and 50 mm/min, respectively. This phase is associated to a martensitic transformation from the orthorhombic to the monoclinic phase. The intensity of this reflection, with indexes  $(\bar{2}01)$  as reported elsewhere,<sup>30,31</sup> increased until elongations reached at about  $\varepsilon = 61, 65.7,$  and  $60.4\%$  (for 1, 10, and 50 mm/min, respectively) and then decreased as deformation continued. The greatest intensity values registered for this monoclinic reflection, for the three deformation rates, are at an elongation closer to the second yield point. This monoclinic peak appeared only in the SS, disappeared after the removal of the stress (see Fig. 2). It is known that the elongation at which the martensitic transformation starts to occur depends on the crystallinity and on the strain rate.<sup>31</sup> This monoclinic reflection has little contribution to the total crystallinity, because its intensity is very small as compared with those of the orthorhombic reflections in all specimens stretched at these deformation rates.

The intensities of crystalline peaks are related through unit-cell structure factors, so their ratios should be constant.<sup>29</sup> In contrast, this was not observed for deformed specimens; it was found that the intensity ratio of (110) to (200) crystal reflections has decrements for elongations beyond the first yield point (see Fig. 2). The variation in this ratio may be caused by the crystal orientation along the stretching direction or the formation of the monoclinic structure. The intensity of the (200) peak grows with elongation respect to that of the (110) peak, and the width of both peaks changed with the deformation. It is well established that decreasing crystallite size, increasing crystallite distortions, and increasing disorientation of the crystallites broaden the reflection.<sup>32</sup> Thus, the width changes of the reflections may indicate changes in the crystallite size.

### Crystallinity

The crystallinity for the three samples stretched at the three deformation rates was calculated in the angular interval from  $15.0^\circ$  to  $27.5^\circ$ , which includes the two very intense (110) and (200) orthorhombic reflections. The variation of the crystallinity associated to these orthorhombic reflections was determined as a function of the elongation. The crystallinity degree ( $\Phi$ ) was calculated as the ratio of the inte-

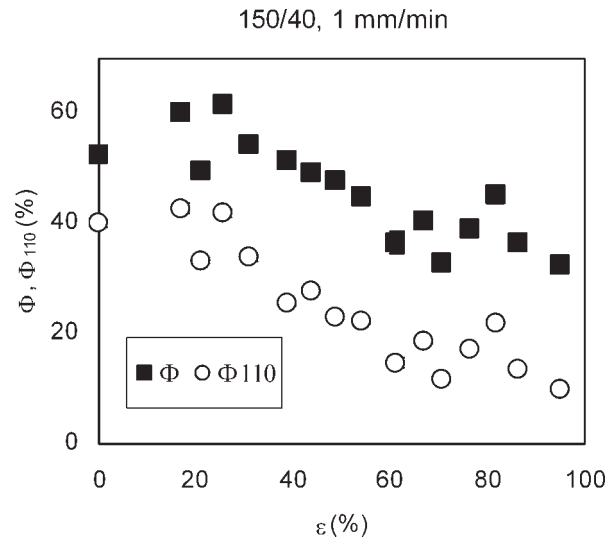


**Figure 3** Degree of crystallinity and the crystallinity associated to the orthorhombic (110) reflection as functions of the elongation. 150/40 specimens stretched at 1 mm/min.

gral of these orthorhombic crystalline peaks over the sum of the integrals of the amorphous and crystalline peaks of both orthorhombic and monoclinic phases. The crystallinity degree was calculated in the standard way<sup>32</sup>; that is, using the relation as follows:

$$\Phi = \frac{A^{110} + A^{200}}{A + A^{110} + A^{200} + A^{\bar{2}01}} \quad (1)$$

where  $A$  and  $A^{hkl}$  are the areas under the amorphous halo and the  $hkl$  reflections, respectively.

The crystallinity values, calculated with the use of eq. (1), are presented in Figures 3–5 for the different stretching rates. The contribution of the (110) reflection ( $\Phi_{110}$ ) to the total crystallinity is also presented in these figures. The total crystallinity is represented by the squared-shape symbols and the  $\Phi_{110}$  contribution by the empty circles. The crystallinity values varied considerably at different strain stages and showed a multistep plot. This behavior is particularly clear in Figure 4, which has a larger number of experimental points. Comparing the behavior of this crystallinity curve to the corresponding ( $\sigma$ - $\varepsilon$ ) curve of Figure 1, the plot in Figure 4 was schematically subdivided into three zones of the elongation. The data of this Figure 4 were taken from the results previously reported.<sup>27</sup> It was called first yield zone (FYZ), that zone with elongations smaller than  $\varepsilon = 35\%$ , valley zone (VZ) that is between 35 and 55%, and second yield zone (SYZ) for elongations higher than 55%, but smaller than the elongation where strain-softening ends and the curve plateau starts. In Figure 4 there are straight lines at the elongation points (35 and 55%), which are the limits of the

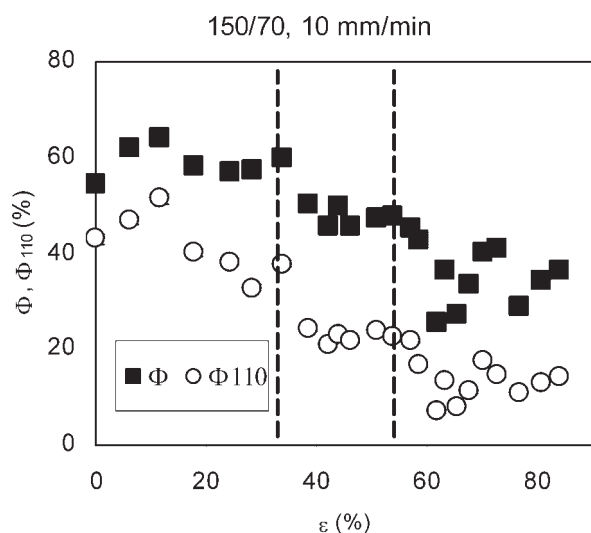


**Figure 4** Degree of crystallinity and the crystallinity associated to the orthorhombic (110) reflection as functions of the elongation. 150/70 specimens stretched at 10 mm/min. Data from Ref. 27.

zones. To identify these zones in Figures 3 and 5 is not easy because there are not sufficient experimental points. However, what is emphasized here is the correlation of the changes in crystallinity and mechanical properties mainly in the SYZ. Although the uncertainty for each point is small, in all cases less than the size of the symbol, the dispersion of the values comes from the nominal stress-strain curves which do not exactly coincide in a same curve for all the stretched specimens at different elongations.

To use as a reference, the crystallinity of the samples without deformation was included in the figures; their values are different to each other because of the processing conditions. In the FYZ, for the three cases, the crystallinity increased at small elongations (below the first yield point), which is associated to the strain-induced crystallization process because on initial deformation the crystallites act as hard inclusions, and the deformation in the material is produced mainly within the amorphous fraction. Figure 4 shows that as the deformation proceeded, the crystallinity value decreased and remained constant in this first zone, within experimental errors. In the VZ the crystallinity shows a significant decrement that may be associated to the fragmentation of the crystalline lamellae, which begins to take place before the occurrence of the second yield point leading to partial transformation of the material into a fibrillar structure.<sup>10</sup> This lamellae fragmentation in turn may cause stress-induced decrystallization. In the SYZ the crystallinity has an additional significant decrement followed by an important increment and then a final decrement, as seen in Figures 3 and 4. The first decrement in this SYZ is associated to par-

tial melting of the smallest or less perfect crystallites. However, the increment can only be associated to a recrystallization process. The final decrement is also generally associated with the neck formation, where a temperature rise may occur (Ref. 2, Chapter 11); with the increase of temperature the decrement of crystallinity is expected. This crystallinity change with the uniaxial deformation is evident for specimens stretched at 1 mm/min whose  $\sigma$ - $\epsilon$  curve exhibits a predominant second yield, for specimens stretched at 10 mm/min the associated  $\sigma$ - $\epsilon$  curve showed that the values of the stress in both yield points were equivalent in magnitude; the shape of the  $\sigma$ - $\epsilon$  curve and the behavior of crystallinity for specimens 180/70 are very similar. The appearance of the second yield point (Fig. 1) is closely related to the increment of crystallinity observed in the SYZ (Figs. 3 and 4). The melting-recrystallization process in the SYZ is more pronounced at the lower and intermediate stretching rates.

The results shown in Figure 4 suggest the validity of a simple scheme for the description of three well-defined zones associated with the first yield, valley, and second yield points which correlate to the elongation intervals observed in the corresponding  $\sigma$ - $\epsilon$  curve of Figure 1. The  $\sigma$ - $\epsilon$  curves of Figure 1 and the  $\Phi$ - $\epsilon$  curves of Figures 3-5, for each stretching rate, follow a qualitative similar pattern. Two most readily observed characteristics are seen in the crystallinity plots. First, the significant decrement that occurs at the very beginning of the SYZ is caused by partial melting of the crystallites; second, the significant increment for elongations in the SYZ is associated to a recrystallization process.

The samples under study have in common the fact that their crystallinity levels are relatively low,

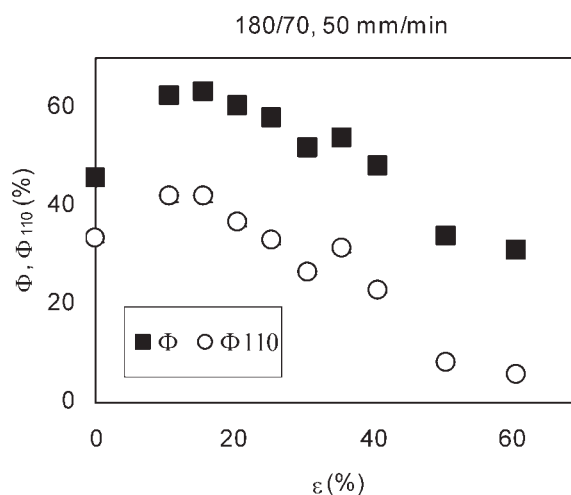


**Figure 5** Degree of crystallinity and the crystallinity associated to the orthorhombic (110) reflection as functions of the elongation. 180/70 specimens stretched at 50 mm/min.

<55%. Therefore, chain units are present that are still potentially crystallizable. Thus, possibility exists that strain-induced crystallization can take place during the tensile deformation. On the other hand, partial melting involves the fusion of the less perfect crystallites. It was proposed that the energy for partial melting comes from the concentration of stress on these less perfect crystallites; thus, it is not necessary for a large temperature rise to take place for partial melting to occur.<sup>4,8</sup> With deformation, the melted material will recrystallize. This crystallization process may be further augmented by the crystallization of some of the initial crystallizable, but not already crystalline units. Some authors have cited evidence for partial melting in the yield region using transmission electron microscopy,<sup>33</sup> whereas partial melting and recrystallization process in the deformation of PE was inferred from neutron scattering experiments.<sup>34</sup>

The crystallinity for the RS, being free of the influence from the monoclinic phase, allow to examine the crystallinity variations because of the exclusive contribution of the mechanical history imposed by the plastic deformation. They show a similar tendency as those of the SS for the different stretching rates, but in a relative minor extent. Those values for the 150/70 sample were reported in a previous work.<sup>27</sup>

It is important to compare the contribution of the orthorhombic (110) reflection to the total crystallinity, because it was reported that the decrease in this equatorial orthorhombic intensity corresponded to the formation of monoclinic material.<sup>16,30</sup> The contribution is shown in Figures 3–5 for the three samples under study. A great parallelism is observed between the behaviors of these data with those corresponding to the total crystallinity. The intensity of the monoclinic ( $\bar{2}01$ ) peak was found to be very small as compared with the orthorhombic (110) peak. The highest monoclinic contribution to the total crystallinity was of  $4.3\% \pm 0.2\%$ ,  $2.94\% \pm 0.08\%$ , and  $2.91\% \pm 0.04\%$  at the elongations mentioned earlier ( $\epsilon = 61.0, 65.7,$  and  $60.4\%$ ) for the three samples. These values in terms of the scale used in these figures are at most equal to the size of the symbol used. Therefore, although the monoclinic material is formed, the significant decrement observed at the start of the SYZ is mainly because of the effect of melting.

The recorded increment of the stress at the second yield point is not a surprise since, in general, the mechanical properties of polymers and, in particular, the yield stress for linear PE increases with the crystallinity degree.<sup>35</sup> Therefore, the detected increase of crystallinity in the SYZ must cause the formation of the second yield maximum, which is confirmed in Figure 1.

The mean crystal size values ( $L_{110}$ ) associated to the (110) reflection for specimens stretched at 10 mm/min, under stress and in the RS were recently reported.<sup>27</sup> They also changed considerably at different strain stages, and allowed the identification of the three zones mentioned earlier. In this reference it was reported that, in the range 60–65% for elongation, where the crystallinity has the highest decrement, the crystallite size had the highest increment. The interpretation was that, as the partial melting is produced on the smallest or less perfect crystallites, the  $L_{110}$  value increased because the crystallites that did not melt have higher size. Therefore, the decrement in the width of this reflection is caused by the increment of the crystallite size.

In this work, it was possible to obtain information that correlates the mechanical behavior of the double yield phenomenon and the variations of the crystallinity level. This experimental evidence indicates that the partial melting–recrystallization process is present in the double yield phenomenon and helps to explain the appearance of the second yield point.

## CONCLUSIONS

The double yield phenomenon was analyzed in samples of LLDPE. Extruded samples processed at three different conditions were uniaxially stretched at 1, 10, and 50 mm/min. The nominal stress–strain curves confirmed that the appearance of this phenomenon depends strongly on the stretching rate, and showed that it occurred much more easily and distinctly at these intermediate and lower stretching rates. In these samples, the stretching rate effect was more important than the effect of the initial crystallinity because the samples covered a small range of initial crystallinity.

The WAXS analysis showed that the double yielding behavior is related to variations of the crystallinity of the stretched specimens at different stages in the course of deformation. This deformation is a multistep process, and at various deformation stages some additional mechanisms are activated.

At relative small elongations, around the first yield point, the crystallinity was increased due to strain-induced crystallization.

In the valley region, between the two yield points, the crystallinity decrement is associated to fragmentation of crystalline lamellae.

In the second yield region the crystallinity again decreased and presented an increment. This behavior is associated to partial melting of smallest or less perfect crystallites followed by recrystallization.

The martensitic transformation from orthorhombic phase to monoclinic phase was observed around the second yield point. But the contribution of the mono-

clinic phase is very small as compared with that of the orthorhombic phase. Therefore, the decrement in the crystallinity contribution of the (110) orthorhombic reflection is mainly because of the partial melting of crystallites, not only to the formation of monoclinic material. These observations are in agreement with a previous report.<sup>27</sup>

The effect of the melting–recrystallization process on the crystallinity behavior is more notorious at the smaller deformation rate where the stress of the second yield point becomes dominant, and at the intermediate deformation rate where the magnitudes of the stress of the two maxima are comparable. At the higher deformation rate where the nominal stress–strain curve shows the first maximum and a hump, the crystallinity–elongation behavior has a similar pattern as the stress–elongation curve.

These findings show that the second yield point is not only associated with the deformation of the crystalline portion, but also a process of partial melting of crystallites followed by a recrystallization takes place.

## References

- O'Connell, P. A.; McKenna, G. B. In *Encyclopedia of Polymer Science and Technology*; Wiley: New York, 2004. Article Online; DOI: 10.1002/0471440264.pst463.
- Ward, I. M.; *Mechanical Properties of Solid Polymers*, 2nd ed.; Wiley: New York, 1990.
- Schultz, J. *Polymer Materials Science*; Prentice-Hall: Englewood Cliffs, 1974.
- Popli, R.; Mandelkern, L. *J Polym Sci Part B: Polym Phys* 1987, 25, 441.
- Seguela, R.; Rietsch, F. *J Mater Sci Lett* 1990, 9, 46.
- Brooks, N. W.; Duckett, R. A.; Ward, I. M. *Polymer* 1992, 33, 1872.
- Séguéla, R.; Darras, O. *J Mater Sci* 1994, 29, 5342.
- Lucas, J. C.; Failla, M. D.; Smith, F. L.; Mandelkern, L.; Peacock, A. *J Polym Eng Sci* 1995, 35, 1117.
- Feijoo, J. L.; Sanchez, J. J.; Muller, A. *J Polym Bull* 1997, 39, 125.
- Gaucher-Miri, V.; Séguéla, R. *Macromolecules* 1997, 30, 1158.
- Schrauwen, B. A. G.; Janssen, R. P. M.; Govaert, L. E.; Maijer, H. E. H. *Macromolecules* 2004, 37, 6069.
- Balsamo, V.; Muller, A. *J Mater Sci Lett* 1993, 12, 1457.
- Plaza, A. R.; Ramos, E.; Manzur, A.; Olayo, R.; Escobar, A. *J Mater Sci* 1997, 32, 549.
- Brooks, N. W. J.; Unwin, A. P.; Duckett, R. A.; Ward, I. M. *J Macromol Sci Phys B* 1995, 34, 29.
- Brooks, N. W.; Unwin, A. P.; Duckett, R. A.; Ward, I. M. *J Polym Sci B: Polym Phys* 1997, 35, 545.
- Butler, M. F.; Donald, A. M.; Ryan, A. *J Polymer* 1997, 38, 5521.
- Muramatsu, S.; Lando, J. B. *Polym Eng Sci* 1995, 35, 1077.
- Shan, G.-F.; Yang, W.; Xie, B.-H.; Li, Z.-M.; Chen, J.; Yang, M.-B. *Polym Test* 2005, 24, 704.
- Shan, G.-F.; Yang, W.; Yang, M.-B.; Xie, B.-H.; Li, Z.-M.; Feng, J.-M. *Polym Test* 2006, 25, 452.
- Shibaya, M.; Ishihara, H.; Yamashita, K.; Yoshihara, N.; Nonomura, C. *Int Polym Proc* 2004, 19, 303.
- Li, Z.-M.; Xie, B.-H.; Yang, S.; Huang, R.; Yang, M.-B. *J Mater Sci* 2004, 39, 433.
- Li, Z.-M.; Huang, C.-G.; Yang, W.; Yang, M.-B.; Huang, R. *Macromol Mater Eng* 2004, 289, 1004.
- Pan, J.-L.; Li, Z.-M.; Ning, N.-Y.; Yang, S. *Macromol Mater Eng* 2006, 291, 477.
- Adhikari, R.; Buschnakowski, M.; Henning, S.; Goerlitz, S.; Huy, T. A.; Lebek, W.; Godehardt, R.; Michler, G. H.; Lach, R.; Geiger, K.; Knoll, K. *Macromol Rapid Commun* 2004, 25, 653.
- Yamada, K.; Takayanagi, M. *J Appl Polym Sci* 1979, 24, 781.
- Spathis, G.; Kontou, E. *J Appl Polym Sci* 2004, 91, 3519.
- Manzur, A.; Rivas, J. I. *J Appl Polym Sci* 2007, 104, 3103.
- Wunderlich, B. *Macromolecular Physics*; Academic Press: New York, 1973; Vol. 1.
- Miller, R. L. In *Encyclopedia of Polymer Science and Technology*; Mark, H. F.; Gaylord, N. G.; Bikales, N. M., Eds.; Wiley: New York, 1966; Vol. 4, p 449.
- Butler, M. F.; Donald, A. M.; Ryan, A. *J Polymer* 1998, 39, 39.
- Butler, M. F.; Donald, A. M.; Bras, W.; Mant, G. R.; Derbyshire, G. E.; Ryan, A. *J Macromolecules* 1995, 28, 6383.
- Alexander, L. E. *X-ray Diffraction Methods in Polymer Science*; Krieger: Huntington, 1979.
- Phillips, P. J.; Philpot, R. J. *Polym Commun* 1986, 27, 307.
- Wignall, G. D.; Wu, W. *Polym Commun* 1983, 24, 354.
- Kennedy, M. A.; Peacock, A. J.; Mandelkern, L. *Macromolecules* 1994, 27, 5297.